Thin Solid Films 519 (2010) 1552–1557

Contents lists available at ScienceDirect

Thin Solid Films

journal homepage: www.elsevier.com/locate/tsf

Pulsed laser deposition of $(MoO_3)_{1-x}(V_2O_5)_x$ thin films: Preparation, characterization and gasochromic studies

Chung-Chieh Chang [a,*], Jiu-Yong Luo [a], Ta-Kun Chen [a], Kuo-Wei Yeh [a], Tzu-Wen Huang [a], Chia-Hao Hsu [a], Wei-Hsiang Chao [a], Chung-Ting Ke [a], Po-Chun Hsu [a], Ming-Jye Wang [b], Mau-Kuen Wu [a]

[a] Institute of Physics, Academia Sinica, Nankang, Taipei, Taiwan
[b] Institute of Astronomy and Astrophysics, Academia Sinica, Nankang, Taipei, Taiwan

ARTICLE INFO

Available online 8 September 2010

Keywords:
Molybdenum oxide
Vanadium oxide gasochromic
Hydrogen sensor
PLD

ABSTRACT

In this study we demonstrate a new composite oxide thin films of $(MoO_3)_{1-x}(V_2O_5)_x$, x = 0, 0.01, 0.03, and 0.05, fabricated by pulsed laser deposition (PLD). The performance of platinum (Pt) catalyst activated hydrogen gas sensor with modified $(MoO_3)_{1-x}(V_2O_5)_x$ thin films were investigated. The thickness of the $(MoO_3)_{1-x}(V_2O_5)_x$ thin film is about 600–650 nm and its surface has a uniform morphology. Our results show that the gasochromic sensors prepared by $(MoO_3)_{0.99}(V_2O_5)_{0.01}$ thin film exhibited excellent hydrogen sensibility. The response and recovery time are in the range of 9–15 min for coloration and bleaching at room temperature under H_2 atmosphere. The results also show that $(MoO_3)_{1-x}(V_2O_5)_x$/Pt (x = 0.01, 0.03, 0.05) thin films perform better gasochromic capability than the pristine MoO_3/Pt sample.

1. Introduction

A gas sensor is a device which can detect the presence of various gases within an area and represent the gas concentration data in a way of electrical or optical signals. In general, gas sensors are used to detect toxic gases (e.g., H_2S, SO_2, CO, NO_X, etc.) and inflammable gases (e.g., CH_4, H_2 and C_2H_5OH, etc.) [1]. Tungsten trioxide (WO_3) thin film is one of the most promising material in gas-sensing study, and a common gasochromic window is composed of a porous, columnar film of WO_3. Recently, semiconducting MoO_3 thin films have been found to act as a promising gas-sensing component because of their sensitivity toward various gases, such as NO, NO_2, CO, NH_3 and H_2 [2,3]. Since then, several techniques have been developed to grow MoO_3 thin films, such as sputtering [4], thermal evaporation [5], sol–gel deposition [6–8], spray pyrolysis technique [9], and chemical vapor deposition [10]. Due to poor electrochemical activity of MoO_3 thin film, therefore, how to overcome those disadvantages of MoO_3 has become an interesting topic [11]. For instance, in order to improve the sensitivity of NH_3 gas detection and the variation of gas-sensing, the MoO_3 thin film surface was further modified with a thin Ti-overlayer and V_2O_5-overlayer, respectively [12]. The reason for choosing V_2O_5 as a doping candidate is because its film has high transparency, high electrochemical activity and stability. In addition, V_2O_5 doping in our samples can increase the transparency of device's initial state. As a result, greater transmittance change (ΔT) can be obtained.

The interaction between V_2O_5 and MoO_3 is unique due to their similar ionic radii and nearly-identical structures in their highest oxidation state. Vanadium-molybdenum oxides have been used as catalysts for the selective oxidation of benzene and other hydrocarbons [13]. A series of cathode materials for lithium-ion batteries with molybdenum–vanadium oxides were synthesized by a high-temperature solid-state method [11]. Their performances show that the cathode materials with V_2O_5 doping have better electrochemical performance. Therefore, improving the structure of MoO_3–V_2O_5, hence the electrochemical properties [14–16], and their interaction mechanism [17–21] have been attracting increasing attention in this decade. However, it is noteworthy that using $(MoO_3)_{1-x}(V_2O_5)_x$ as a gas-sensing material has not been reported so far.

In general, a conventional thin film sensor requires a top-capped layer of catalyst on which H_2 dissociated into two H atoms. Among all, platinum (Pt) [1,22] and palladium (Pd) [23,24] are the most common catalysts. Therefore, a bronze, $H_xMo^{VI}_{1-x}Mo^{V}_{x}O_3$, forms when H atoms transfer from the catalyst onto the MoO_3 surface [1,25,26]. The chemical reaction mechanism was simply proposed as the following:

$$H_2 \xrightarrow{Pt} 2H \quad (1)$$

$$xH + MoO_3 \rightarrow \underset{\text{(colorless)}}{H_xMo^{VI}_{1-x}Mo^{V}_{x}O_3} \quad \underset{\text{(blue)}}{} \quad (2)$$

Having a hydrogen atom inserts into MoO_3, the oxidation states of molybdenum has reduced from +6 to +5; hence, the color of MoO_3 changes from transparent to blue. As a result, the quantity of hydrogen gas can be estimated from the changes of the electrochemistry or

* Corresponding author. Tel.: +886 2 27880058#8403; fax: +886 2 2783 4187.
E-mail address: ccchang1978@phys.sinica.edu.tw (C.-C. Chang).

0040-6090/$ – see front matter © 2010 Elsevier B.V. All rights reserved.
doi:10.1016/j.tsf.2010.09.003

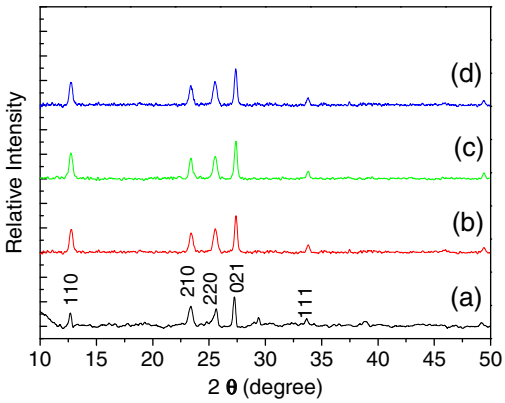

Fig. 1. X-ray diffraction patterns of $(MoO_3)_{1-x}(V_2O_5)_x$ film: (a) x = 0, (b) x = 0.01, (c) x = 0.03, and (d) x = 0.05.

photochemistry of MoO_3. This gasochromic reaction is reversible so it is possible to detect the hydrogen gas or to apply on windows [26]. In this paper, we have $(MoO_3)_{1-x}(V_2O_5)_x$ thin films with x = 0, 0.01, 0.03, and 0.05 prepared by PLD method. The preparation and characterization of thin films was reported and the effect of V_2O_5 additive on the thin film structure, morphology and gasochromic behavior was thoroughly investigated.

2. Experimentals

$(MoO_3)_{1-x}(V_2O_5)_x$ x = 0, 0.01, 0.03, and 0.05 composite thin films were fabricated by PLD method [27,28]. In order to make a good PLD target, high purity (5 N) of $(MoO_3)_{1-x}(V_2O_5)_x$ x = 0, 0.01, 0.03, and 0.05 with 8 g total weight were prepared and each one was well mixed for 3 h by a steady powder mixing machine. Then they were compressed in a form of pellet with 25 mm diameter and 5 mm height and sintered at 600 °C for 12 h under the atmosphere [29]. Microscope slide glasses were used as their substrates. The substrates were cut into 1×1 cm^2. All substrates were cleaned with detergent soap, alcohol and de-ionized water before PLD. A λ = 248 nm laser beam was provided by the KrF laser (Lambda Physik LPX Pro). The repetition rate is 2 Hz and laser intensity of about 5 ~ 6 J/cm^2. The deposition rate of thin film is about 0.05 nm/shot. The deposition chamber contained 3 Torr oxygen partial pressure and the temperature of glass substrates were kept at 250 °C. After deposition, the thin films were post-annealed in synthetic air at 300 °C for 1 h. A layer of platinum with 10 nm thickness was sputtered on the $(MoO_3)_{1-x}(V_2O_5)_x$ thin film to complete a sensor device structure [1], and all experiments were performed at room temperature.

Surface morphology, thicknesses and elemental compositions of $(MoO_3)_{1-x}(V_2O_5)_x$/Pt thin films were examined by a Field-Emission Scanning Electron Microscope with Energy Dispersive Spectrometer (FE-SEM-EDS, HITACHI S4200, Japan). The crystal structure and phase identification of the thin films were investigated by an X-ray diffractometry (XRD, PANalytical X'pert PRO MPD Diffractometer, Netherlands Cu K_α radiation) with a grazing incidence of angle 2°. The accelerating voltage and the applied current were 45 kV and 40 mA, respectively. The colorations of hydrogen gas detection at room temperature were measured by an UV–vis spectrophotometer (BAL2000, Ocean Optics, Inc., USA).

3. Results and discussion

3.1. Structural properties

PLD technique can be employed as a fast and reliable process to synthesize $(MoO_3)_{1-x}(V_2O_5)_x$ (x = 0, 0.01, 0.03, and 0.05) thin films. The characterization of the resulting thin films has been investigated using XRD, as shown in Fig. 1. We observe clear peaks corresponding to the expected MoO_3 XRD reference data (JCPDS Card No. 5-0508). The orthorhombic phase of MoO_3 thin films is shown in Fig. 1a. The intensities of (110), (210), (220), and (021) Bragg peaks for MoO_3/V_2O_5 dopant films are much stronger than those undoped films. This implies that the grain size of MoO_3 crystallite increases with the amount of V-doping. It can be seen that an increase in V_2O_5 doping resulted in an intensity enhancement and narrowing of (110) peak, indicating a progressive growth of crystallites. Using the Scherrer equation,

$$d = \frac{k\lambda}{\beta\cos(\theta)} \tag{3}$$

where β (radians) is the full-width of half-maximum at 2θ of 12.7°, k is a constant (0.89), λ is the X-ray wavelength (1.541 Å for Cu K_α), d is

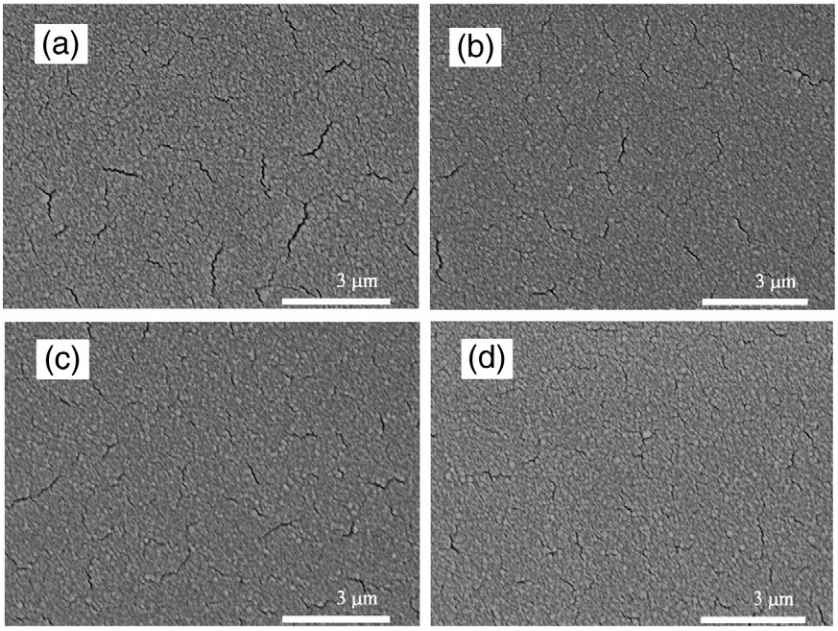

Fig. 2. The FE-SEM images of $(MoO_3)_{1-x}(V_2O_5)_x$ as-deposited film: (a) x = 0, (b) x = 0.01, (c) x = 0.03, and (d) x = 0.05.

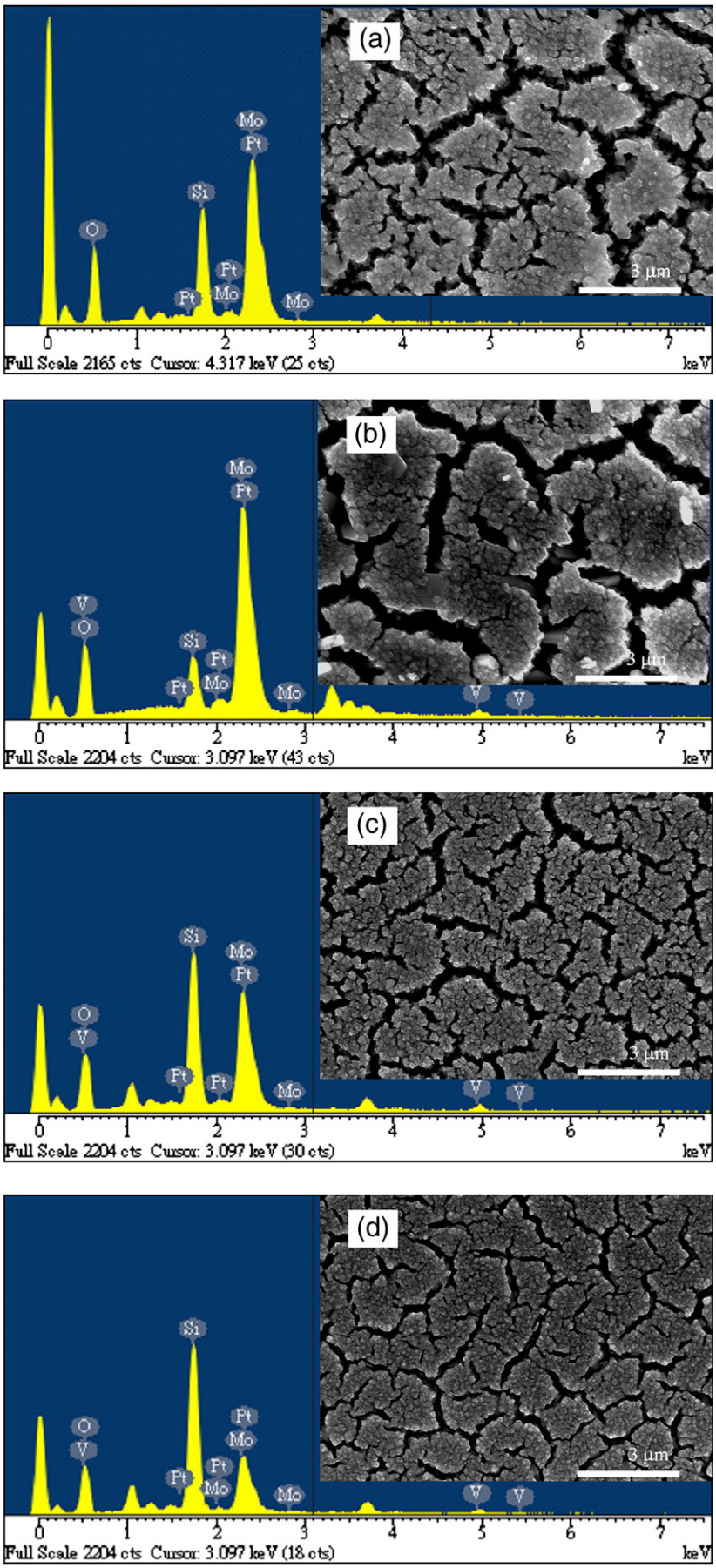

Fig. 3. The FE-SEM images and EDS spectrums of $(MoO_3)_{1-x}(V_2O_5)_x$ film after annealing: (a) x = 0, (b) x = 0.01, (c) x = 0.03, and (d) x = 0.05.

Table 1
Element compositions of $(MoO_3)_{1-x}(V_2O_5)_x$/Pt films: (a) x = 0, (b) x = 0.01, (c) x = 0.03, and (d) x = 0.05.

	Mo (L)	V(K)	Pt (M)	In(L)	Sn(L)	Si(K)	O(K)
(a)	14.93	0	0.37	4.71	0.72	7.77	71.50
(b)	17.78	1.00	0.57	3.05	0.56	4.62	72.43
(c)	16.73	1.58	0.44	3.37	0.77	6.34	70.77
(d)	11.37	1.43	0.37	5.24	0.65	9.89	71.05

Atomic%.

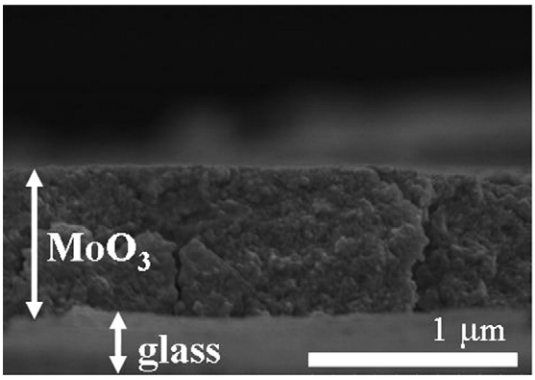

Fig. 4. The FE-SEM images of the cross-section of $(MoO_3)_{1-x}(V_2O_5)_x$ film (x = 0).

the particle diameter and θ is the angle of the diffraction peak (degrees), the crystallite sizes of samples (a) to (d) are estimated to be 17.5 nm, 19.7 nm, 20.8 nm, and 21.1 nm, respectively.

Fig. 2 shows topographical images of $(MoO_3)_{1-x}(V_2O_5)_x$ as-deposited thin films. The surface is almost covered by small grains and gaps on the surface were formed during growth. Fig. 3 shows the topographical images and EDS analysis of a series of $(MoO_3)_{1-x}(V_2O_5)_x$/Pt thin films. It is clear that the size of grains and gaps have increased after annealing, hence, the gas-sensing area has increased as well. Table 1 summarizes the EDS quantitative analysis results of all samples. The existence of molybdenum, vanadium and platinum in the prepared films was confirmed. It is noted that the high oxygen content in the results was due to the influence of the glass substrate, supported by the existence of Si in the EDS analysis.

The thickness of all thin films prepared in this study was estimated to be approximately 600–650 nm by cross-section FE-SEM images. The FE-SEM image of the cross-section of $(MoO_3)_{1-x}(V_2O_5)_x$ (x = 0) film is presented in Fig. 4. It shows that the MoO_3 thin film had an

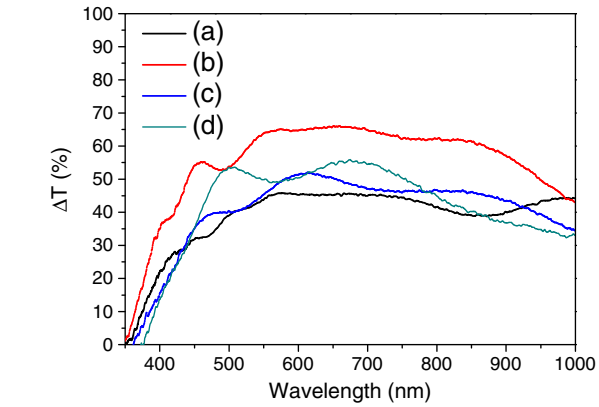

Fig. 6. Transmittance changes (ΔT) of $(MoO_3)_{1-x}(V_2O_5)_x$/Pt thin films after exposure to H_2 gas: (a) x = 0, (b) x = 0.01, (c) x = 0.03, and (d) x = 0.05.

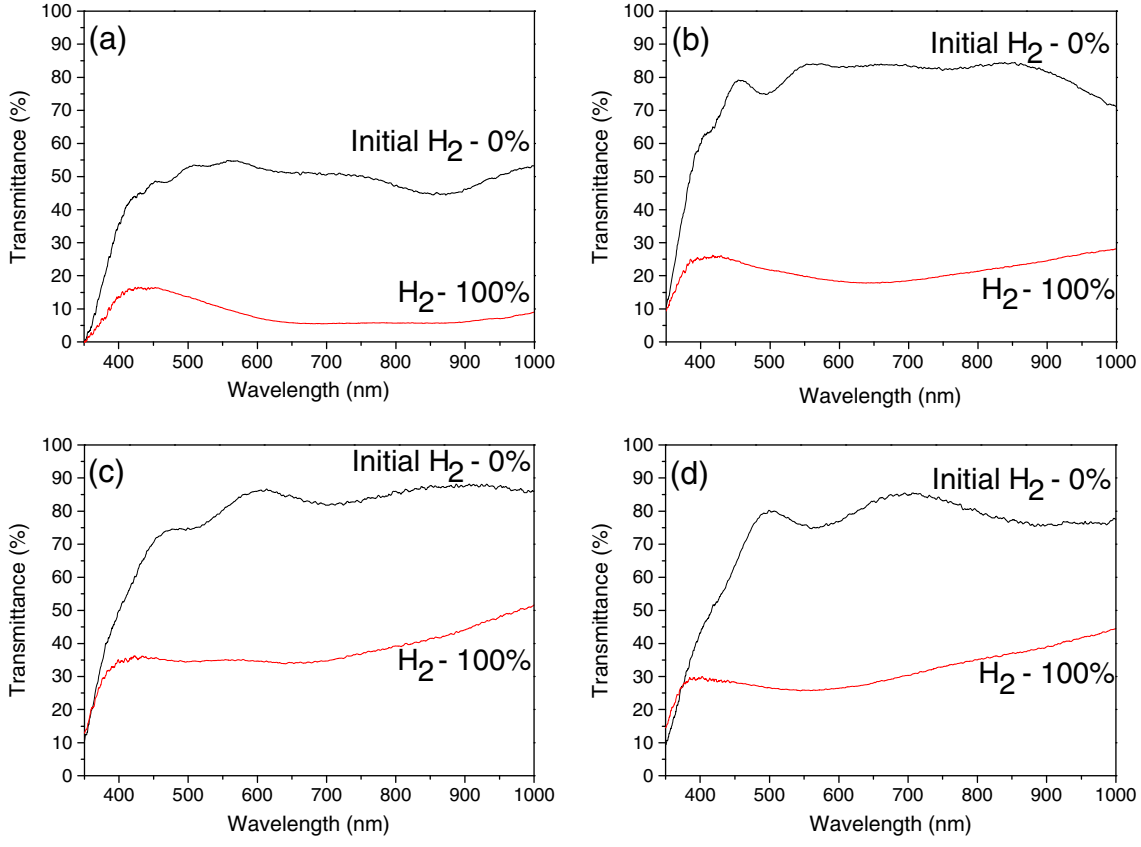

Fig. 5. In-situ UV–vis spectra of the gasochromic sensor after exposure to H_2 gas.

uniform structure and was composed of granular particles with a small grain size.

3.2. Gasochromic properties

Gasochromism occurs when hydrogen atoms transfer from the catalyst layer onto the molybdenum trioxide surface and alter the film's optical absorption. The transmittance spectra of the gasochromic device after hydrogen gas exposure are shown in Fig. 5. $(MoO_3)_{1-x}(V_2O_5)_x$/Pt (x = 0.01, 0.03, 0.05) samples exhibit higher transmittance than conventional MoO_3/Pt sample does. The $(MoO_3)_{0.99}(V_2O_5)_{0.01}$/Pt thin film has the highest transmittance and the best intensity of coloration. It is also shown in Fig. 5 that the transmittance spectra of the initial state and the bleached state almost overlap. This confirms that the device's coloration and bleaching reactions are reversible.

Furthermore, we also found that the transmittance change (ΔT) of $(MoO_3)_{1-x}(V_2O_5)_x$/Pt gasochromic device increases with wavelength. It can be observed that the average of transmittance change (ΔT) of $(MoO_3)_{1-x}(V_2O_5)_x$/Pt (x = 0.01, 0.03, 0.05) samples is much higher than that of pristine MoO_3 sample as illustrated in Fig. 6. At visible region, the longer the wavelength is, the higher the sensitivity will be. $(MoO_3)_{0.99}(V_2O_5)_{0.01}$/Pt sample has the highest transmittance change (ΔT). However, for the sake of avoiding possible heating effect in longer wavelength, we choose 450 nm, 550 nm, and 650 nm for comparison in the following discussion.

We used optical transmittance responses to evaluate coloration dynamics of our devices. Fig. 7 shows the optical transmittance responses of gasochromic devices exposed to H_2 at 450 nm, 550 nm, and 650 nm wavelength. As shown in Fig. 6, the $(MoO_3)_{0.99}(V_2O_5)_{0.01}$/Pt film has the shortest response time and highest transmittance change (ΔT) in the range of 53.8–65.6%.

Moreover, both the transmittance change (ΔT) and response time performance of these sensors at 650 nm are better than those at 550 nm and 450 nm. Therefore, the optical transmittance data at 650 nm looks promising to monitor the sensing ability of the gasochromic sensor prepared in this study.

Table 2
The response (t_{color}), recovery time (t_{bleach}) and transmittance changes (ΔT) of $(MoO_3)_{1-x}(V_2O_5)_x$/Pt films: (a) x = 0, (b) x = 0.01, (c) x = 0.03, and (d) x = 0.05.

(a)	t_{color}, min	12	11	11
	t_{bleach}, min	18	17	17
	ΔT,%	31.8	43.6	45.2
(b)	t_{color}, min	9	8.7	8.7
	t_{bleach}, min	15	14	14
	ΔT,%	53.6	63.9	65.8
(c)	t_{color}, min	10	9.5	9.5
	t_{bleach}, min	15	15	15
	ΔT,%	35.2	45.6	50.5
(d)	t_{color}, min	13.5	13	13
	t_{bleach}, min	13	12.5	12.5
	ΔT,%	32.5	50.1	54.7

The performance characteristics of the sensors are summarized in Table 2. It is shown that both the response and recovery times are in the range of 9–15 min at room temperature in H_2 gas. The results also show that $(MoO_3)_{1-x}(V_2O_5)_x$/Pt (x = 0.01, 0.03, 0.05) samples have better gasochromic properties than the pristine MoO_3/Pt sample does. Furthermore, in order to compete with the conventional WO_3 film sensors, we wish to shorten the response and recovery times within a range of a minute in the future.

4. Conclusion

In this paper, a series of $(MoO_3)_{1-x}(V_2O_5)_x$ (x = 0, 0.01, 0.03, 0.05) thin films were successfully synthesized by PLD. Results show that the gasochromic performance of the MoO_3 thin film is improved with V_2O_5 doping. The thickness of the $(MoO_3)_{1-x}(V_2O_5)_x$ thin film

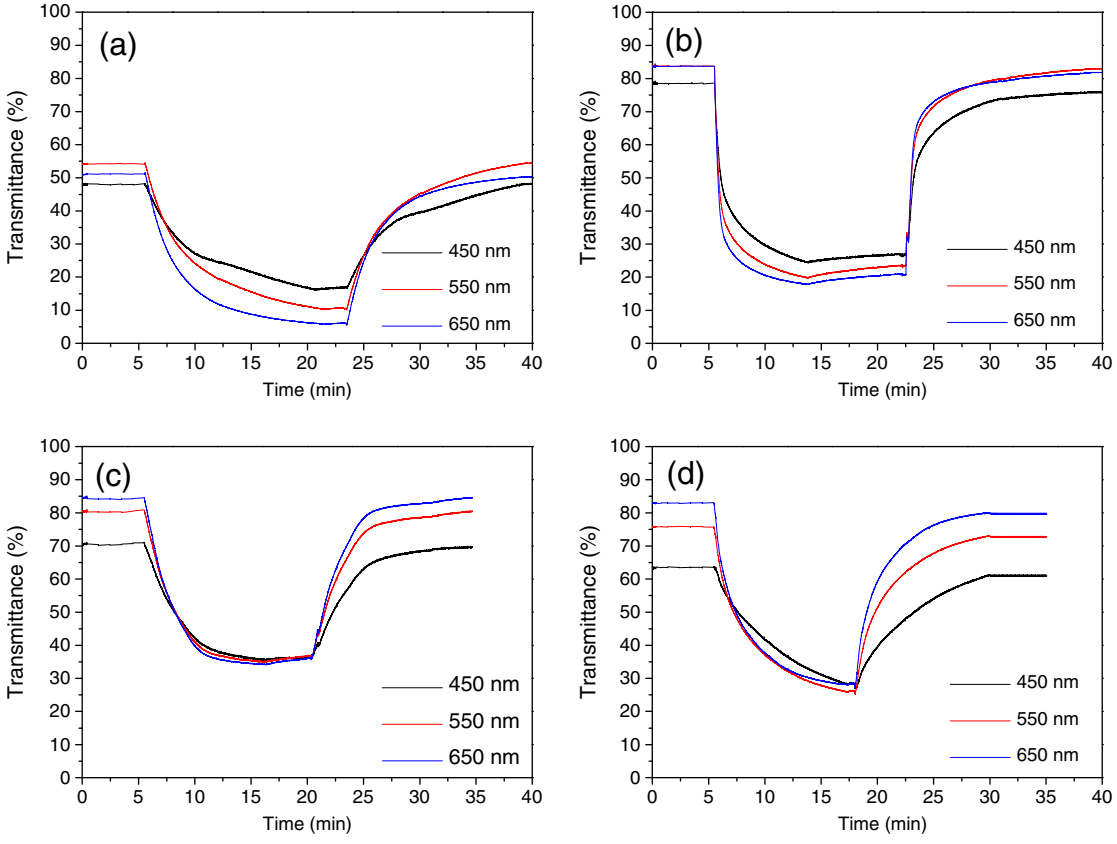

Fig. 7. Optical transmittance responses of the $(MoO_3)_{1-x}(V_2O_5)_x$/Pt thin films after exposure to H_2 gas: (a) x = 0, (b) x = 0.01, (c) x = 0.03, and (d) x = 0.05.

is about 600–650 nm and the surface exhibits an uniform morphology. A good hydrogen sensor can be prepared by sputtering a layer of Pt over the $(MoO_3)_{1-x}(V_2O_5)_x$ (x = 0, 0.01, 0.03, 0.05) thin films. The $(MoO_3)_{0.99}(V_2O_5)_{0.01}$/Pt film has the shortest response time and highest transmittance change (ΔT) in the range of 53.8–65.6%, which is very similar to the conventional WO_3 film sensors performance. Finally, we have shown that the performance of these gasochromic $(MoO_3)_{1-x}(V2O_5)_x$/Pt (x = 0.01, 0.03, 0.05) thin films compares better than the conventional MoO_3/Pt thin films.

Acknowledgement

This work was founded by National Science Council of Taiwan under Grant NSC-96-2112-M-001-026-MY3 and NSC-98-2119-M-001-025.

References

[1] W.J. Shiu, C.C. Chan, C.H. Peng, C.C. Chang, Thin Solid Films 516 (2–4) (2007) 407.
[2] D. Mutschall, K. Holzner, E. Obermeier, Sens. Actuators B 35 (36) (1996) 320.
[3] M. Ferroni, V. Guidi, G. Martinelli, M. Sacerdoti, P. Nelli, G. Sberveglieri, Sens. Actuators B 48 (1998) 285.
[4] M. Kharrizi, L. Kullman, C.G. Granqvist, Solar Energy Mater. Solar Cells 53 (1998) 349.
[5] N. Miyata, T. Suzuki, R. Ohyama, Thin Solid Films 281 (282) (1996) 218.
[6] T. Brezesinski, J. Wang, S.H. Tolbert, B. Dunn, Nat. Mater. 9 (2010) 146.
[7] C.S. Hsu, C.C. Chan, H.T. Huang, C.H. Peng, W.C. Hsu, Thin Solid Films 516 (2008) 4839.
[8] N. Ozer, C.M. Lampert, Thin Solid Films 349 (1999) 205.
[9] P.R. Patil, P.S. Patil, Thin Solid Films 382 (2001) 13.
[10] D. Barreca, P. Nelli, G.A. Rizzi, G. Sberveglieri, E. Tondello, Conference Proceedings of SAA'99 National Meeting on Sensors for Advanced Applications, 54, 1997, p. 49.
[11] X. Wei, L. Jiao, S. Liu, J. Sun, W. Peng, H. Gao, Y. Si, H. Yuan, J. Alloy Compounds 486 (2009) 627.
[12] C. Imawan, F. Solzbacher, H. Steffes, E. Obermeier, Sens. Actuators B 77 (2001) 346.
[13] A. Bielanski, M. Najbar, Appl. Catal. A General 157 (1997) 223.
[14] Ch.V. Subba Reddy, Y.Y. Qi, W. Jin, Q.Y. Zhu, Z.R. Deng, W. Chen, Sun-il Mho, J. Solid State Electrochem. 11 (2007) 1239.
[15] Ch.V. Subba Reddy, E.H. Walker, C. Wen, Sun-il Mho, J. Power Sources 183 (2008) 330.
[16] R.Y. Lin, J.F. Elliott, J. Alloys Compd. 321 (2001) 261.
[17] Y.S. Kim, H.J. Ahn, H.S. Shim, T.Y. Seong, Solid State Ionics 177 (2006) 1323.
[18] K.V. Madhuri, B.S. Naidu, O.M. Hussian, Mater. Chem. Phys. 77 (2003) 22.
[19] V.A. Zazhigalov, S.V. Khalameida, N.S. Litvin, I.V. Bacherikova, J. Stoch, L. Depero, Kinet. Catal. 49 (2008) 692.
[20] J.R. Sohn, J.S. Han, J.S. Lim, Mater. Chem. Phys. 91 (2005) 558.
[21] A. Neiman, S. Barsanov, J. Solid State Electrochem. 5 (2001) 382.
[22] C.C. Chan, W.C. Hsu, C.C. Chang, C.S. Hsu, Sens. Actuators B Chem. 145 (2010) 691.
[23] B. Orel, U. Opara Krašovec, N. Grošelj, M. Kosec, G. Drazic, R. Reisfeld, J. Sol. Gel Sci. Technol. 14 (1999) 291.
[24] S. Sekimoto, H. Nakagawa, S. Okazaki, K. Fukuda, S. Asakura, T. Shigemori, S. Takahashi, Sens. Actuators, B, Chem. 66 (2000) 142.
[25] M. Zayat, R. Reisfeld, H. Minti, B. Orel, F. Svegl, J. Sol. Gel Sci. Technol. 11 (1998) 161.
[26] V. Wittwer, M. Datz, J. Ell, A. Georg, W. Graf, G. Walze, Sol. Energy Mater. Sol. Cells 84 (2004) 305.
[27] M.J. Wang, J.Y. Luo, T.W. Huang, H.H. Chang, T.K. Chen, F.C. Hsu, C.T. Wu, P.M. Wu, A.M. Chang, M.K. Wu, PRL 103 (2009) 117002.
[28] M.K. Wu, F.C. Hsu, K.W. Yeh, T.W. Huang, J.Y. Luo, M.J. Wang, H.H. Chang, T.K. Chen, S.M. Rao, B.H. Mok, Phys. C 469 (2009) 340.
[29] M. Ranjbar, S.M. Mahdavi, A. Iraji, Sol. Energy Mater. Sol. Cells 92 (2008) 878.